Published in final edited form as:
Curr Eye Res. 2012 September ; 37(9): 761–769. doi:10.3109/02713683.2012.676699.

Nonclassical Innervation Patterns In Mammalian Extraocular Muscles

Roberta M. da Silva Costa, M.D., Ph.D.[1], **Jennifer Kung, B.A.**[1], **Vadims Poukens, M.D., Ph.D.**[1], and **Joseph L. Demer, M.D., Ph.D.**[1,2,3,4]

[1]Department of Ophthalmology, University of California, Los Angeles

[2]Neuroscience, University of California, Los Angeles

[3]Bioengineering Interdepartmental Programs, University of California, Los Angeles

[4]Neurology Department, University of California, Los Angeles

Abstract

Purpose—The abducens (CN6) and oculomotor (CN3) nerves (nn) enter target extraocular muscles (EOMs) via their global surfaces; the trochlear (CN4) nerve enters the superior oblique (SO) muscle on its orbital surface. Motor nn are classically described as entering the EOMs in their middle thirds. We investigated EOM innervation that does not follow the classic pattern.

Methods—Intact, whole orbits of two humans and one each monkey, cow, and rabbit were paraffin embedded, serially sectioned in coronal plane, and prepared with Masson's trichrome and by choline acetyltransferase (ChAT) immunohistochemistry. Nerves innervating EOMs were traced from the orbital apex toward the scleral insertion, and some were reconstructed in three dimensions.

Results—Classical motor nn positive for ChAT entered rectus and SO EOMs and coursed anteriorly, without usually exhibiting recurrent branches. In every orbit, nonclassical (NC) nn entered each EOM well posterior to classical motor nn. These NC nn entered and arborized in the posterior EOMs, mainly within the orbital layer (OL), but often traveled into the global layer or entered an adjacent EOM. Other NC nn originated in the orbital apex and entered each EOM through its orbital surface, ultimately anastomosing with classical motor nn. Mixed sensory and motor nn interconnected EOM spindles.

Conclusions—EOMs exhibit a previously undescribed pattern of NC innervation originating in the proximal orbit that partially joins branches of the classical motor nn. This NC innervation appears preferential for the OL, and may have mixed supplemental motor and/or proprioceptive functions, perhaps depending upon species. The origin of the NC innervation is currently unknown.

Keywords

cranial nerve; eye movement; extra-ocular muscle; spindle

The rich structural complexity of extraocular muscles (EOMs) is poorly understood. The EOMs are unusual among muscles because they exhibit rare characteristics including a plethora of fiber types, diverse morphology, histochemistry, gene expression, and

Address for Correspondence and Reprint Requests: Joseph L. Demer, M.D., Ph.D., Jules Stein Eye Institute, 100 Stein Plaza, UCLA, Los Angeles, CA 90095-7002. (310) 825-5931 voice; (310) 206-7826 fax; jld@ucla.edu.

Declaration of Interest: The authors report no conflicts of interest.

innervation patterns[1–3]. An example of this unusual structure is the compartmentalized organization into an inner global layer (GL) contiguous with the tendon and inserting on the eyeball, and an outer orbital layer (OL) that inserts on a connective tissue ring forming the EOM pulley[4]. The two layers contain different fiber types with distinct activation patterns during eye movements[5]. Another singular feature of EOMs is the presence of both twitch fibers with a single endplate zone (SIFs), and also non-twitch fibers with multiple endplate zones (MIFs), features otherwise absent from mammalian muscles[2, 6]. In addition, EOM myosin composition differs significantly from all other skeletal muscles, including the presence of the unusual α-cardiac myosin, and persistence of embryonic and neonatal myosin isoforms in adults[6]. Myosin heavy chain expression in EOMs is highly heterogeneous, with longitudinal variation within single fibers, and cross-sectional variation of each isoform[7–9]. All these features reflect the complex contractile profiles of EOMs that execute a diverse behavioral repertoire ranging from quick phases and saccades, to slow phase and tracking movements, as well as sustained fixations.

At present the peripheral innervation of EOMs is incompletely understood. The innervation to the EOMs includes the motor cranial nerves (nn), sensory branches of the trigeminal n, and autonomic nn[10]. The oculomotor (CN3) and trochlear (CN4) cranial nn originate in the midbrain; the abducens (CN6) cranial n originates in the pons[10]. All three classical motor cranial nn to the EOMs enter the orbit via the superior orbital fissure. CN3 and CN6 pass through the common tendonous ring and proceed distally to enter their target rectus EOMs from their global surfaces. A branch of the inferior division of CN3 enters the posterior surface of the inferior oblique EOM. CN4 remains outside the common tendonous ring and enters the superior oblique EOM from its superior orbital surface. Autonomic nerves (nn) supply multiple structures in the orbit. Sympathetic nn enter the human orbit via the ophthalmic and maxillary divisions of the trigeminal n. (CN5), and a plexus surrounding the ophthalmic artery[11]. Branches of the nasociliary, frontal, lacrimal, and maxillary nn convey sympathetic nn to join the classical motor branches of CN3, CN4, and CN6 in the proximal orbit, and presumably convey branches to a small number of catecholaminergic neurons in the ciliary ganglion[11]. Sympathetic projections appear mainly to supply orbital blood vessels, smooth muscles, the uveal tract, and lacrimal gland. Parasympathetic innervation in the human orbit originates in the ciliary and pterygopalatine ganglia, and projects mainly to supply the uveal tract, blood vessels, and orbital smooth muscles[12]. However, in the rat, lesion of the ipsilateral superior cervical ganglion decreased the density of cholinesterase-positive nn in Müller's orbital smooth muscle, indicating that the superior cervical ganglion also contributes to cholinergic innervation[13]. Aside from projections to intramuscular blood vessels, autonomic innervation within striated EOMs has not been considered significant.

Although classical descriptions of the cranial nn supplying EOMs are fundamental topics in basic biology texts[14], there is some evidence suggesting motor innervation supplementing the classical nn. For example some EOM fibers, particularly in the OL, are remarkably resistant to lesions of the classical motor cranial nn originating in the CN3, CN4, and CN6 nuclei[15–17]. Porter *et al.* found progressive reduction in medial rectus fiber cross section to 50% of control values by 112 days following CN3 section. This was followed by hypertrophy to about 50% greater than control by 6 mos., when re-innervation occurred from an unknown, presumably non-CN3 source[18]. The occasional finding of clusters of hypertrophic superior oblique (SO) fibers following CN4 neurectomy in monkeys also suggests the possibility of supplemental motor innervation to the SO from sources other than the classical CN4[17].

The EOMs probably also receive sensory innervation, but the anatomy and physiology of EOM proprioception remains controversial. At least two types of proprioceptors are found in EOMs of some species: muscle spindles and Golgi tendon organs[19, 20]. Additionally,

palisade endings have historically been considered to be proprioceptive, although recent findings indicate that the palisades have motor features[21], or perhaps sensorimotor function[20]. Proprioceptive input from EOMs influences ocular motor control[22]. Although the existence of these proprioceptive signals is well established, controversy remains concerning the site of primary afferent terminals in the EOM, and their anatomic pathway to the central nervous system[20]. Gentle and Ruskell described Wallerian degeneration following intracranial section of CN3 or the ophthalmic division of CN5 in monkeys, but showed that the numbers of CN5 ophthalmic division sensory fibers transferring to the classical motor nn to the inferior rectus (IR) and superior rectus (SR) are insufficient to meet the requirements of proprioception[23]. These authors proposed that some or perhaps all of those nn that transfer serve functions other than proprioception[23].

The foregoing considerations suggest that there may exist non-autonomic nn projections to the EOMs that supplement the classical branches of CN3, CN4, and CN6. The present report describes non-classical (NC) nn observed in intact, whole orbits of several mammals, including primates. We considered NC nn to be those entering EOMs via routes other than the main branches of CN3, CN4, and CN6. We also excluded the presumably autonomic nn that are intimately associated with intramuscular blood vessels or innervate orbital smooth muscles. While it was not possible to follow the NC innervation to its source or sources in these specimens, we sought to trace NC nn as far as possible to distinguish it from classical innervation pathways.

METHODS

Animal orbits were obtained through tissue sharing after humane sacrifice according to approved procedures performed at other institutions. No living humans or animals were employed. An orbit from a 17 month old (H7) human male was obtained in conformity with legal requirements from a tissue bank (IIAM, Scranton, PA) and submitted to decalcification, dehydration and paraffin embedding. The same procedures were performed in a macaque monkey, a rabbit, and a cow. Serial sections from the whole orbits were obtained at 10 μm thickness in the quasi-coronal plane perpendicular to the long orbital axis, mounted on 50 × 75 mm glass slides, stained at approximately 100 μm intervals with Masson's trichrome (MT) or occasionally with van Gieson's elastin stain[24]. This procedure requires 3,000 – 6,000 sections per orbit, depending upon orbit size. Based upon features of interest, additional selected sections at smaller intervals were stained with MT or immunostained for choline acetyltransferase (ChAT) (Millipore, Temecula, CA) diluted 1:100 in phosphate buffer, incubated with rabbit anti-goat IgG (Vector, Burlingame, CA) as a secondary antibody, reacted with Vectastain ABC reagent complex (Vector), and visualized with diaminobenzidine (Vector). Digital micrographs were prepared using a light microscope (Eclipse E800, Nikon, Tokyo, Japan) fitted with a digital camera (Nikon D1X) using 0.5X – 100X objectives.

Since the inferior rectus (IR) muscle generally has the highest number of spindles of all EOM[25], the deep orbital portion of a human IR was studied in detail. A field containing abundant spindles was selected for tridimensional reconstruction. To avoid inclusion of "false" spindles, strict criteria were employed to confirm true spindles[26, 27]. Spindles were required to exhibit complete capsules without gaps, to extend 150–1800 μm in length, and contain fibers smaller than neighboring extrafusal fibers. Serial sections were used to trace the spindles and small nn connecting them.

To reconstruct small nn deep in the orbits, typically 20 – 50 sections around each n were photographed with 40× magnification. Contiguous fields of the same section were stacked into layers using *Photoshop* CS4 (Adobe Systems, San Jose, CA) to form a single merged

file. Next, the image from the deepest slide in the orbit was used as a template to rotate and translate subsequent section images into alignment. Using this image stack, each spindle and its associated nn were traced to create profiles, which were arbitrarily assigned different colors to facilitate following them through the superimposed layers. The traced profiles of the spindles and associated nn were reconstructed in three dimensions (3D) using the program *ImageJ* (Rasband, W.S., U. S. National Institutes of Health, Bethesda, MD, http://rsb.info.nih.gov/ij/, 1997–2009) running on an 8-processor Mac Pro Computer (Apple Computer, Cupertino, CA) with 32 Gb random access memory. It was necessary to reduce image resolution in some cases as multi-view, 3D reconstruction over long anatomical distances is highly intensive of computer memory.

RESULTS

Classical EOM Innervation

Branches of classical motor nn, CN3, CN4, and CN6, were prominent and readily identified in every orbit studied. Axons in these nn were large and strongly positive for cholinergic staining. These provided a positive control for cholinergic innervation in each orbit. These could be easily traced from the orbital apex as they coursed anteriorly and arborized within EOMs. Large cell bodies within the ciliary ganglion were also positive for ChAT, providing an additional positive control for cholinergic autonomic innervation. Axons in the optic nerve (ON) were negative for ChAT, providing a negative control for the ChAT immunohistochemistry in each orbit. With exception of CN4, all motor nn enter on the global surface near the border between the posterior and middle thirds of the EOMs, dividing into several branches anteriorly within the muscle. There was little or no evidence of recurrent branches that coursed posteriorly from the nerve entry point.

Nonclassical EOM Innervation

NC nn were found in the EOMs of all species evaluated. Typically, bundles containing multiple fibers entered each EOM well posterior to the point that classical motor nn reach the EOMs. This entry site was frequently in a location so posterior in the orbit that the corresponding classical motor n had not yet divided from a single trunk (Figs. 1 and 2). The NC nn considered here were not the fine, autonomic nerves that occur, usually as single fibers, dispersed widely in the orbit in the vicinity of orbital non-vascular and vascular smooth muscles, and to myofibroblasts.

Unlike the classical motor nn that enter the EOMs through the GL, most of these NC nn entered and arborized mainly within the OL (Fig. 3). The NC n in Fig. 3 was traced as it coursed anteriorly along the orbital surface of the bovine LR from a source more than 5.1 cm posterior to the corneal surface, and then turned at a right angle to enter transversely in a region of abundant spindles. Some of these nn exhibited progressively increasing cross sections as they coursed anteriorly, suggesting that some were joined by fibers originating anteriorly.

Other NC nn originated in the orbital apex and entered each EOM through its orbital surface, giving several branches that ultimately anastomosed with small branches from classical motor nn (Fig. 4). The NC n illustrated in Fig. 4 originated deep in the orbit outside the common tendonous ring, penetrated the dense connective tissue of the ring, and traveled anteriorly along the orbital surface of the SR distinct from any innervation to the levator palpebrae superioris muscle. The NC n approached another small NC n of uncertain origin, then along with that smaller NC n, entered the SR orbital layer, where it divided into a small branch arborizing terminally among the fibers of the medial SR. A larger branch not only arborized among the SR fibers, but that also had an anastomosis with a classical

intramuscular motor n. When present, anastomotic connections between NC and classical nn occurred in the OL, as between small branches in human SR (Fig. 4), human IR, and bovine LR. Other larger branches joined the classic motor nn near their entry into the GL. In some cases they anastomosed with the classic motor n (Fig. 4E). In this high power view of a NC n cross section the mean fiber diameter was measured at 3.3 ± 0.57 μm (SD) of a sample of 23 fibers. Anastamotic connections like that shown in Fig. 4 were observed in human SR and LR, and in bovine LR. Other large NC branches joined the classic motor nn near their entry into the GL. Thus, in addition to the NC fibers that entered the orbital side of the EOM, a set that entered the global side was also observed. These differed from the classical fibers in that they arborized near their entry point, instead of extending distally like classic fibers upon entry.

Some NC n branches traveled by unusual routes. For example, they extended between adjacent EOMs, as observed in one human orbit (Fig. 5). The ChAT positive n illustrated in Fig. 5 split into several small branches within both EOMs (IR and MR), and one of these branches joined CN3 far anteriorly. In the rabbit SR, ChAT reactive NC nn entered the EOM from the deep orbit through its GL, traveled anteriorly to the OL, and then traveled further anteriorly to join the classical motor n in the GL. This was established by tracing of serial sections for the NC n illustrated in Fig. 6.

Spindles

A small region of the inferior orbital part of the human MR was photographed and examined carefully to locate all 13 spindles found there. Spindles varied in length from 150 to 1,360 μm (median 800 μm). Maximum widths at the equator varied from 49 to 182 μm (median 112 μm). A network of NC nn was found interconnecting the spindles. In some of them the nn entered the spindle capsule and connected with a small n bundle within the spindle before continuing onward. After that, these nn split into variable numbers of branches directed to other EOM fascicles, other spindles, or joined n. branches that were derived from different locations. More distally, after forming a neural network, these small nn joined the large branches of CN3 that were observed to enter the EOM from the opposite GL side. A 3D reconstruction of these structures is shown in (Fig. 7).

DISCUSSION

We report here that EOMs receive a previously undescribed pattern of NC innervation that partially joins branches of the classical motor nn. We also demonstrated the presence of a neural network connecting human EOM spindles. At least some of the axons in these n bundles are cholinergic based upon ChAT immunoreactivity. This suggests that the nn interconnecting the spindles include a motor component, as would be appropriate to the proprioceptive organs that spindles are believed to be[25].

Classical descriptions of EOM innervation indicate that the major n. branches, except CN4, enter the EOMs on their global surfaces, approximately between the posterior and middle third of their lengths, and thereafter course anteriorly with little or no recurrent arborization by intramuscular n trunks (Fig. 8).[28] Conversely, the NC n fibers described here frequently entered the EOMs through the OL, on the opposite side from the classical nn entry, and joined the EOM more proximally than classical fibers. These NC fibers were observed in all species studied. The anatomical differences between the classical and NC nn are diagrammed in Fig. 8. Some NC nn entered the EOM via the GL, but nevertheless displayed a very posterior entry into the EOMs not contiguous with the classical n trunks.

It is likely that the NC nn described here were overlooked in prior investigations for methodological reasons. They are smaller and less well-defined than the classical n trunks,

and would easily be destroyed or confused with connective tissues during dissection of individual EOMs. The present study of NC nn required careful tracing in serial sections of whole orbits undisturbed by dissection. This method of preparation and examination of whole orbits is more laborious than gross dissection. Serial histological examination of excised individual EOMs is less laborious, but mechanical isolation of individual EOMs makes it impossible to appreciate their relationships to small NC nerves entering very close to the EOM origins or from the orbital surfaces.

The central source of the NC innervation is currently unknown. The nn interconnecting the spindles are likely to be proprioceptive, and have both sensory and motor elements in agreement with the observation that some but not all, of the fibers were ChAT-positive. Nonclassical nn that did not interconnect spindles may have supplemental motor functions, but are probably not autonomic based upon the large diameter of their axons. Most of the non-classical nn were thicker proximally, and grew thinner as they branched and extended distally. This pattern suggests that they do not represent recurrent branches of the classical nn.

Orbital smooth muscle fibers, most of which are located in the anterior orbit, receive numerous small autonomic nerves from the pterygopalatine, ciliary, and superior cervical ganglia[29]. While our previous tracing studies of smooth muscle innervation did not include reconstructions from serial sections, they did identify fine cholinergic, catecholaminergic, and nitroxidergic nn external to the striated EOMs[29]. These autonomic projections were predominantly very fine single fibers located anteriorly in the orbit in the vicinity of smooth muscle cells or myofibroblasts, and are therefore unlikely to be the same as the NC nn investigated in the current study, which instead occur posteriorly in bundles containing at least some larger fibers. There was no sign of connectivity of the NC nn with the main parasympathetic source of cholinergic innervation to the orbit, the ciliary ganglion[29]. Similarly, the NC nn did not travel towards the inferior orbital fissure, the location of the pterygopalatine ganglion, the other parasympathetic source of cholinergic innervation to the orbit[29].

Nonclassical EOM innervation might explain the perplexing results of experimental denervation. Destruction of classical nn to EOMs does not produce denervation atrophy in all EOM fibers. Morphological examinations of MR and IR following CN3 denervation in dogs suggested that atrophy occurs only in the singly innervated fibers; the size of the multiply innervated fibers in both the GL and OL was not significantly affected[16]. In fact, the proportion of multiply innervated fibers in the OL of the denervated EOM increased. Likewise, CN4 denervation in monkey produces predominantly SO GL atrophy with relative OL sparing[17], and preservation of the peripheral cap motor neurons of the trochlear nucleus (Demer, *et al.*, unpublished observation). Some have speculated that the resistance of EOMs to denervation atrophy arises from rapid reinnervation by their classical motor nn[18], or their unique myosin content[16]. However, it is alternatively possible that OL resistance to denervation might be due to NC nn that are mainly present in this layer, perhaps arising from a segregated motor neuron pool. In rabbit SR, apparently normal and completely degenerated fibers were observed side by side for at least three weeks following CN3 section, suggesting the presence of an independent secondary source of innervation.[15] While the possibility of sympathetic innervation of classically denervated EOM fibers has been proposed[14, 30], the NC nn observed here also appear to be reasonable candidates for secondary innervation.

Proprioceptive signals from EOMs can be found in central structures, including the trigeminal nucleus, vestibular nucleus, and somatosensory cortex. These signals may be important for oculomotor control and visual sensory development[14, 31]. Although the

existence of these proprioceptive signals is well established, there is still controversy over the site of primary afferent terminals and their anatomic pathways to the brain. In cats, it is claimed that EOM proprioceptive fibers exit the orbit exclusively with the classic CN3, CN4 and CN6[32]. Up to 10% of fibers in the distal feline CN3 and CN4 joined CN5, as well as 6% of CN6 fibers. In addition, 3 – 5% of fibers in CN3 degenerated following intracranial section of CN5[33]. Anastomoses between CN4 and CN5 in the cavernous sinus have been observed in goats[34]. In humans, similar anastomoses have also been described, not only between CN4 and CN5, but also between CN6 and CN5[33]. However, although the classical EOM nn have been classified as sensorimotor, a complete description of the paths of entry of afferent fibers into these nn has not been made in any species[14]. The NC nn described here may, in part, represent CN5 fibers that never joined CN3, CN4 and CN6, or ones that joined and then separated as the main n entered the orbit.

Spindles are encapsulated proprioceptors present in mammalian skeletal muscles. Their structure and distribution in EOMs are well described[25, 27, 33]. Spindles are prominent in the EOMs of humans, sheep and other ruminants, but are found only rarely or not at all in monkeys, baboons, and cats[33]. However, not all species exhibit spindles in EOMs, so NC nn must have additional or alternative functions to spindle innervation, depending upon species. Muscle spindles are supplied by both motor and sensory terminals[27]. Here we verified the presence of a neuronal network connecting human EOM spindles that is located in the deep portion of the EOM, posterior to entry of the classical motor n. The spindle nn ultimately joined the classical CN, which may be the source of motor or sensory innervation to the spindles. It is possible that fibers transfer from motor n to CN5 in the superior orbital fissure or in cavernous sinus where, because of the tight packing of tissues, it is difficult to observe connections by dissection[14].

The present use of whole orbital specimens facilitates the study of tissue relationships that might otherwise be overlooked. In humans and ruminants, NC nn in the EOMs might represent a possible interface between the afferent and efferent systems deep in the orbit, and explain otherwise paradoxical survival of EOM fibers following destruction of classical motor innervation[15, 17, 18].

Acknowledgments

Support: Supported by U.S. Public Health Service, National Eye Institute: grants EY08313 and EY00331, and Research to Prevent Blindness. J. Demer is Leonard Apt Professor of Ophthalmology.

References

1. Brueckner JK, Ashby LP, Prichard JR, Porter JD. Vestibulo-ocular pathways modulate extraocular muscle myosin expression patterns. Cell Tissue Res. 1999; 295:477–484. [PubMed: 10022967]
2. Lennerstrand G. Strabismus and eye muscle function. Acta Ophthalmol Scand. 2007; 85:71–723.
3. Wieczorek DF, Periasamy M, Butler-Browne GS, Whalen RG, Nadal-Ginard B. Co-expression of multiple myosin heavy chain genes, in addition to a tissue-specific one, in extraocular musculature. J Cell Biol. 1985; 101:618–629. [PubMed: 3894379]
4. Demer JL. Pivotal role of orbital connective tissues in binocular alignment and strabismus. The Friedenwald lecture. Invest Ophthalmol Vis Sci. 2004; 45:729–738. [PubMed: 14985282]
5. Collins, CC. The human oculomotor control system. In: Lennerstrand, G.; Bach-y-Rita, P., editors. Basic Mechanisms of Ocular Motility and Their Clinical Implications. New York: Pergamon; 1975. p. 145-180.
6. Porter JD. Extraocular muscle: cellular adaptations for a diverse functional repertoire. Ann NY Acad Sci. 2002; 956:7–16. [PubMed: 11960789]
7. Zhou Y, Liu D, Kaminski HJ. Myosin heavy chain expression in mouse extraocular muscle: more complex than expected. Inv Ophthalmol Vis Sci. 2010; 51:6355–6363.

8. McLoon LK, Rios L, Wirtschafter JD. Complex three-dimensional patterns of myosin isoform expression: Differences between and within specific extraocular muscles. J Musc Res Cell Motil. 1999; 20:771–783.
9. Moncman CL, Andrade ME, Andrade FH. Postnatal changes in the developing rat extraocular muscles. Inv Ophtalmol Vis Sci. 2011; 52:3962–3969.
10. Demer, JL. Extraocular Muscles. In: Tasman, W.; Jaeger, EA., editors. Duane's Clinical Ophthalmology. Hagerstown, MD: Lipincott; 2009. p. 1-30.
11. Thakker MJ, Huang J, Possin DE, et al. Human orbital sympathetic nerve pathways. Oph Plastic Reconstr Surg. 2008; 24:360–366.
12. Baljet B, van dWF, Otto AJ. Autonomic pathways in the orbit of the human fetus and the rhesus monkey. Doc Ophthalmol. 1989; 72:247–264. [PubMed: 2625087]
13. Yamashita T, Honjin R. Fine structure, origin, and distribution of the autonomic nerve endings in the tarsal muscle in the eyelid of the mouse. Cell Tissue Res. 1982; 222:459–465. [PubMed: 7083312]
14. Tarkhan AA. The innervation of the extrinsic ocular muscles. J Anat. 1934; 68:293–313. [PubMed: 17104478]
15. Cheng-Minoda K, Ozawa T, Breinin GM. Ultrastructural changes in rabbit extraocular muscles after oculomotor nerve section. Invest Ophthalmol Vis Sci. 1968; 7:599–616.
16. Christiansen SP, Baker S, Madhat M, Terrell B. Type-specific changes in fiber morphometry following denervation of canine extraocular muscle. Exp Mol Pathol. 1992; 56:87–95. [PubMed: 1587343]
17. Demer JL, Poukens V, Ying H, Shan X, Tian J, Zee DS. Effects of intracranial trochlear neurectomy on the structure of the primate superior oblique muscle. Invest Ophthalmol Vis Sci. 2010; 51:3485–3493. [PubMed: 20164458]
18. Porter JD, Burns LA, McMahon EJ. Denervation of primate extraocular muscle. A unique pattern of structural alterations. Invest Ophthalmol Vis Sci. 1989; 30:1894–1908. [PubMed: 2759804]
19. Buttner-Ennever JA, Eberhorn A, Horn AKE. Motor and sensory innervation of extraocular eye muscles. Ann N Y Acad Sci. 2003; 1004:40–49. [PubMed: 14662446]
20. Leinbacher K, Mustari M, Ying HS, Buttner-Ennever J, Horn AK. Do palisade endings in extraocular muscles arise from neurons in the motor nuclei? Inv Ophthalmol Vis Sci. 2011; 52:2510–2519.
21. Zimmermann L, May PJ, Pastor AM, Streicher J, Blumer R. Evidence that the extraocular motor nuclei innervate monkey palisade endings. Neurosci Lett. 2011; 489:89–93. [PubMed: 21138754]
22. Weir CR, Knox PC, Dutton GN. Does extraocular muscle proprioception influence oculomotor control? Br J Ophthalmol. 2000; 84:1071–1074. [PubMed: 10966971]
23. Gentle A, Ruskell G. Pathway of the primary afferent nerve fibres serving proprioception in monkey extraocular muscles. Ophthal Physiol Optics. 1997; 17:225–231.
24. Sheehan, DC.; Hrapchak, BB. Theory and Practice of Histotechnology. St. Louis: Mosby; 1973. p. 95-116.
25. Lukas JR, Aigner M, Blumer R, Heinzl H, Mayr R. Number and distribution of neuromuscular spindles in human extraocular muscles. Invest Ophthalmol Vis Sci. 1994; 35:4317–4327. [PubMed: 8002252]
26. Blumer R, Konakci KZ, Brugger PC, et al. Muscle spindles and Golgi tendon organs in bovine calf extraocular muscle studied by means of double-fluorescent labeling, electron microscopy, and three-dimensional reconstruction. Exp Eye Res. 2003; 77:447–462. [PubMed: 12957144]
27. Ruskell GL. The fine structure of human extraocular muscle spindles and their potential proprioceptive capacity. J Anat. 1989; 167:199–214. [PubMed: 2630535]
28. Erdogmus S, Govsa F, Celik S. Innervation features of the extraocular muscles. J Craniofac Surg. 2007; 18:1439–1446. [PubMed: 17993897]
29. Demer JL, Poukens V, Miller JM, Micevych P. Innervation of extraocular pulley smooth muscle in monkeys and humans. Invest Ophthalmol Vis Sci. 1997; 38:1774–1785. [PubMed: 9286266]
30. Baker RS, Millett AJ, Young AB, Markesbery WR. Effects of chronic denervation on the histology of canine extraocular muscle. Invest Ophthalmol Vis Sci. 1982; 22:701–705. [PubMed: 7076415]

31. Wang N, May PJ. Peripheral muscle targets and central projections of the mesencephalic trigeminal nucleus in macaque monkeys. Anat Rec (Hoboken). 2008; 291:974–987. [PubMed: 18461596]

32. Sivanandasingham P. Peripheral pathway of proprioceptive fibres from feline extra-ocular muscles. I. A histological study. Acta Anat (Basel). 1978; 100:173–184. [PubMed: 74182]

33. Ruskell GL. Extraocular muscle proprioceptors and proprioception. Prog Ret Eye Res. 1999; 18:269–291.

34. Whitteridge D. A separate afferent nerve supply from the extra-ocular muscles of goats. Q J Exp Physiol Cogn Med Sci. 1955; 40:331–336. [PubMed: 13280813]

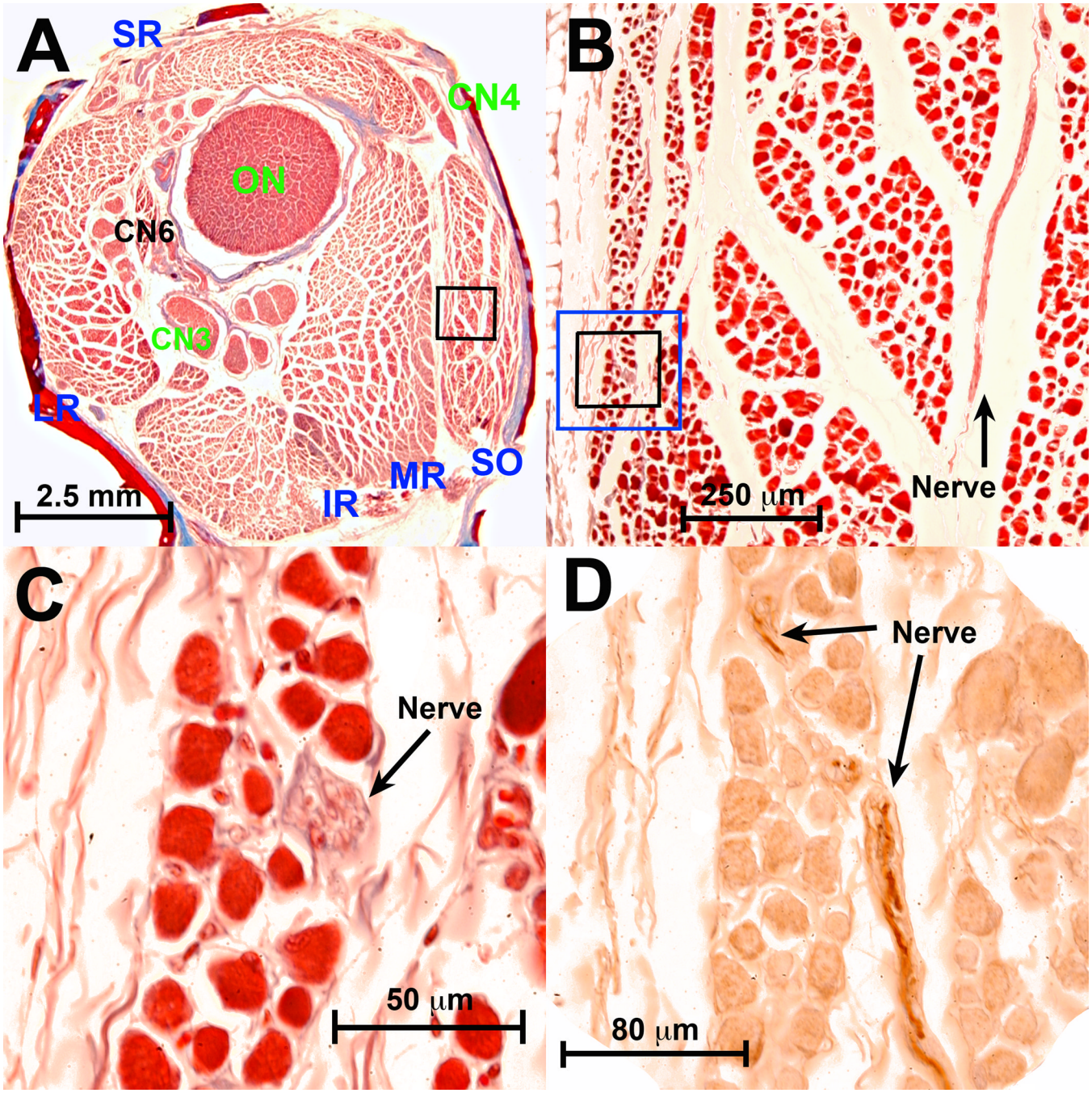

Fig. 1.

Nonclassical (NC) nn in monkey superior oblique (SO) posterior to entry of the classical trochlear n (CN4). **A.** Low power Masson trichrome stain of whole orbit. **B.** Magnified region in black rectangle in A shows NC n oriented within the plane of section in the orbital layer of the SO. Masson trichrome. **C.** Region in black rectangle from B shows NC n oriented perpendicular to plane of section. Masson trichrome. **D.** Region of blue rectangle (in serial section 30 μm anterior) in B shows dark brown choline acetyltransferase (ChAT) immunoreactivity in NC n. extending within the plane of section to the n. bundle in C. Fine motor endplates in EOM fibers are also reactive for ChAT, and orbital layer fibers have a

diffuse weak positivity for ChAT. CN3 – inferior division of oculomotor n. CN6 – abducens n. IR – inferior rectus. LR – lateral rectus. MR – medial rectus. ON – optic nerve. SR – superior rectus.

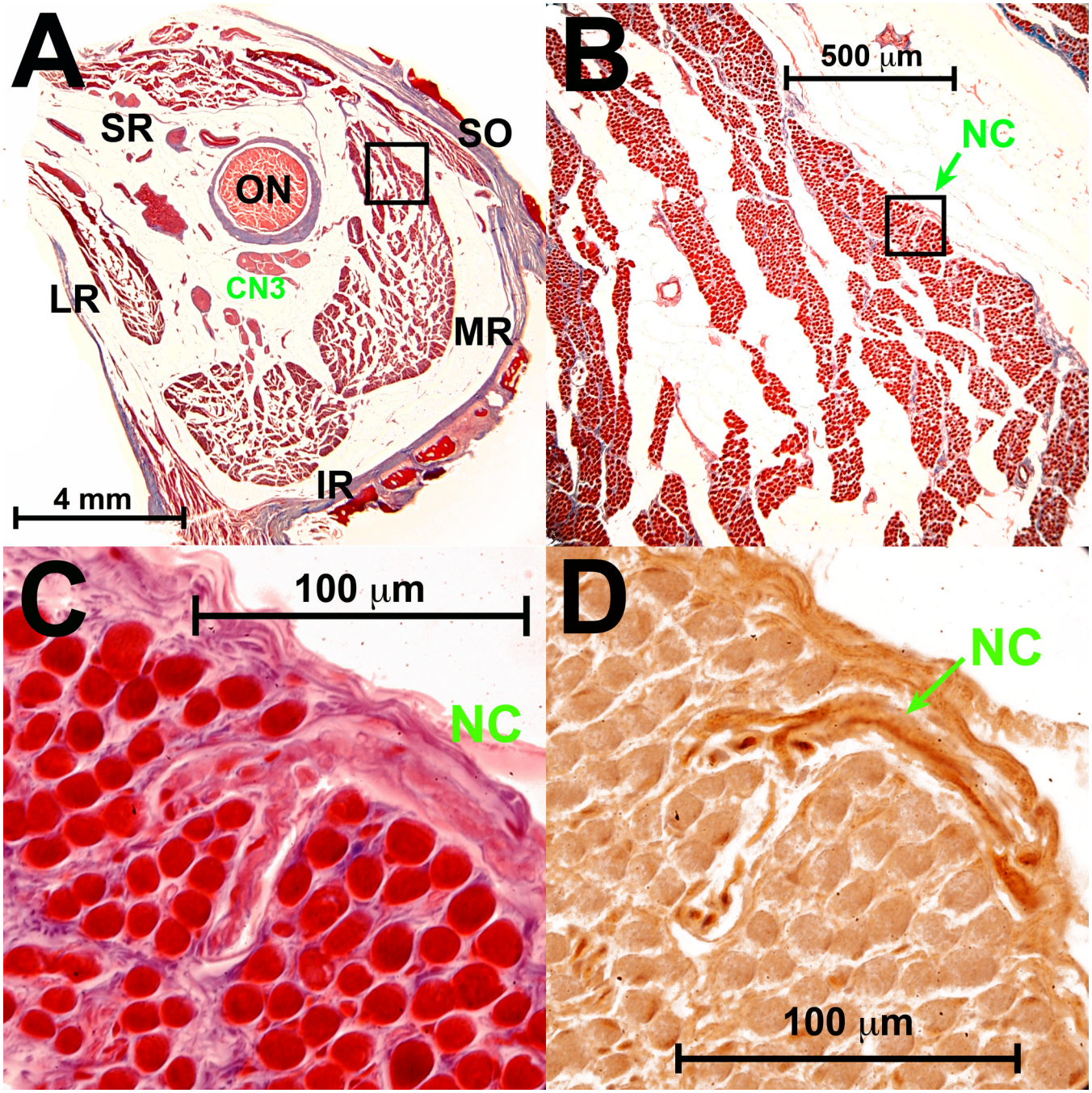

Fig. 2.

Deep human orbit. **A.** Masson trichrome stain shows CN3 is still external to the global surface of the medial rectus (MR) muscle. **B.** Magnified view of region outlined by black square in A, showing entry of small nonclassical (NC) nerve into superior orbital surface of MR. C. High power view of region outlined by black square in B, showing entry and bifurcation of NC nerve within MR orbital layer. D. Adjacent serial section region outlined by black square in B, showing choline acetyltransferase (ChAT) immunoreactivity (brown) in some axons of the NC n. ON - optic n. CN3 – inferior division of oculomotor n. Abbreviations as in Fig. 1.

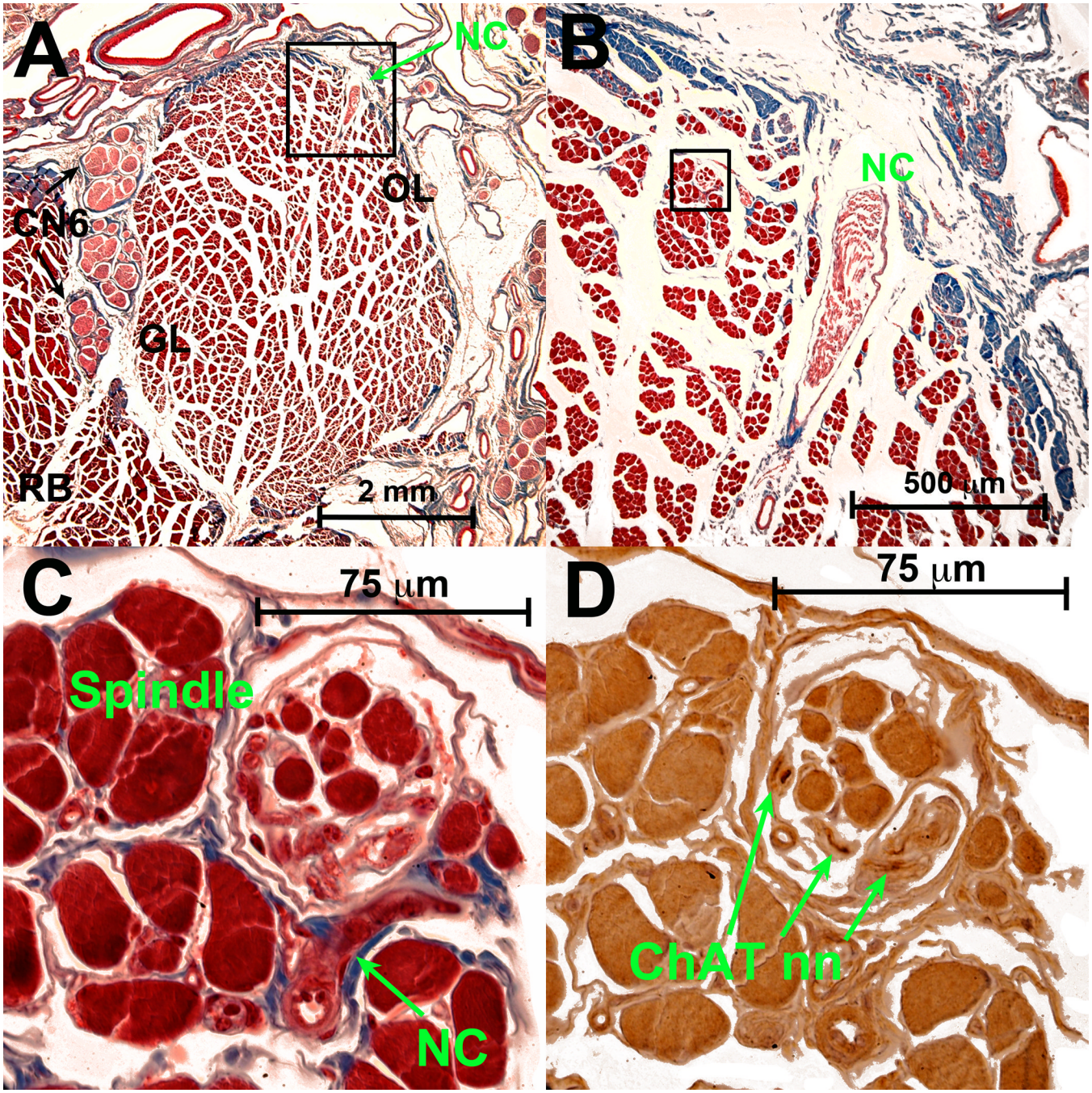

Fig. 3.

Bovine LR muscle. **A.** Low power Masson trichrome stain shows classical CN6 that has repeatedly divided on the global (left) LR surface as it courses anteriorly to enter on the global surface (not shown) of the global layer (GL). Nonclassical (NC) n. enters LR orbital layer (OL) from its superior orbital surface in the deep orbit. **B.** Magnified view of region in black square shown in A, demonstrating entry of NC n. **C.** High power view of region in black square shown in B, demonstrating NC n. entry into a spindle, distinct from the blood vessel seen below it. D. ChAT in nearby serial section demonstrates dark brown

immunoreactivity of some axons in NC nerve in the spindle shown in C. RB – retractor bulbi muscle. Other abbreviations as in Fig. 1.

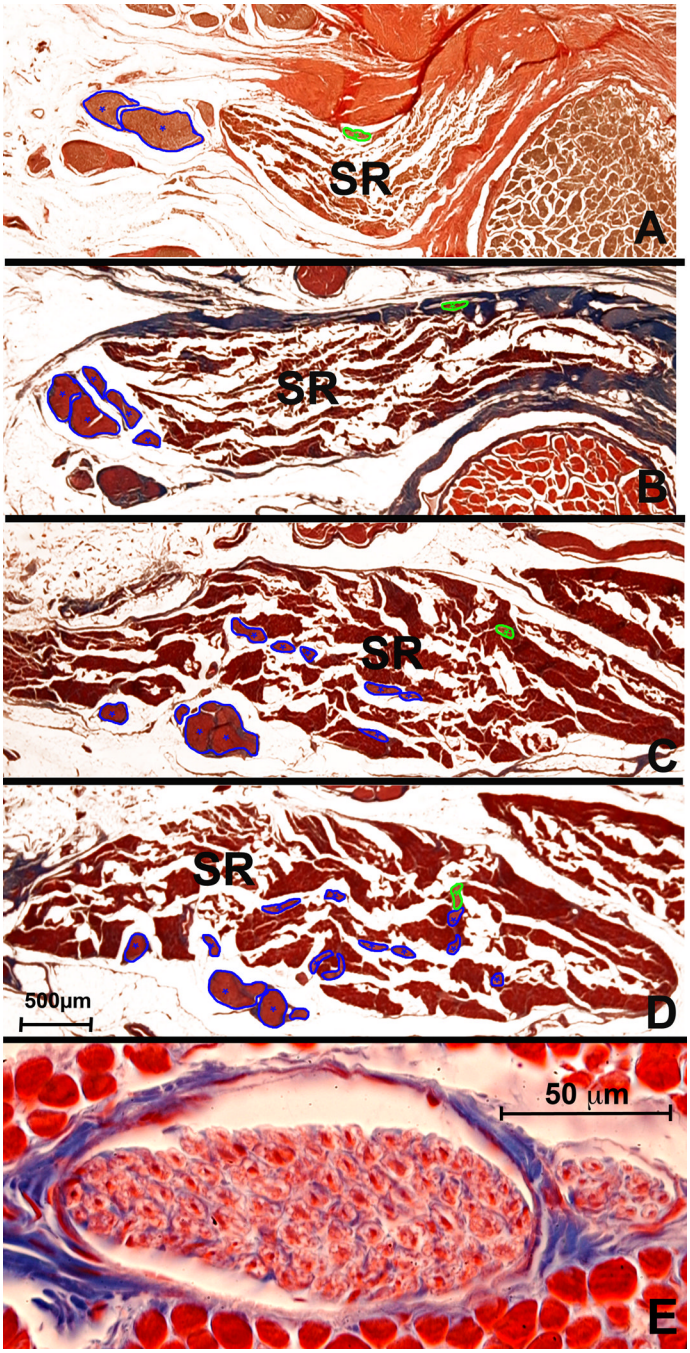

Fig. 4.

Human superior rectus (SR). Panels A – D from posterior to anterior at low power. Classical motor n. from superior division of CN3 (marked in blue), enters the EOM but is joined by a ChAT positive NC n. (marked in green) entering the SR more posteriorly through its orbital surface. E. High power cross section of anterior portion of NC nerve and its smaller branch (right) showing predominance of large fibers. A. Van Gieson stain. B – E. Masson trichrome stain. 500 µm scale bar for A – D. 50 µm scale bar for E.

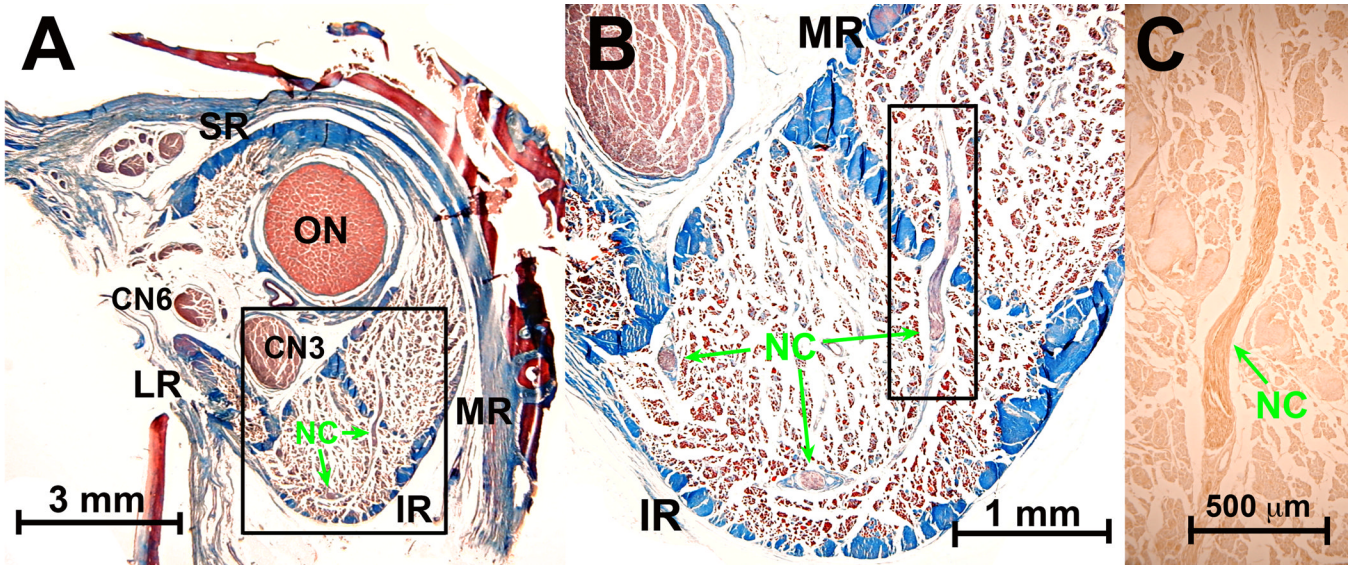

Fig. 5.

Apex of human orbit near the rectus origin at the annulus of Zinn, 37.81 mm posterior to corneal surface. A. Masson trichrome shows n. branch that appeared in deep sections and traveled from inferior rectus (IR) to medial rectus (MR) muscle. A small branch from this n. entered the main trunk of CN3 before CN3 gave any branch to any EOM. B. Higher magnification of region in A outlined by rectangle demonstrates that NC n travels through the collagenous septum separating the IR ad MR. C. Darker brown central ChAT immunostaining in nearby serial section of region demarcated by rectangle in B demonstrates positive brown staining of NC n. Abbreviations as in Fig. 1.

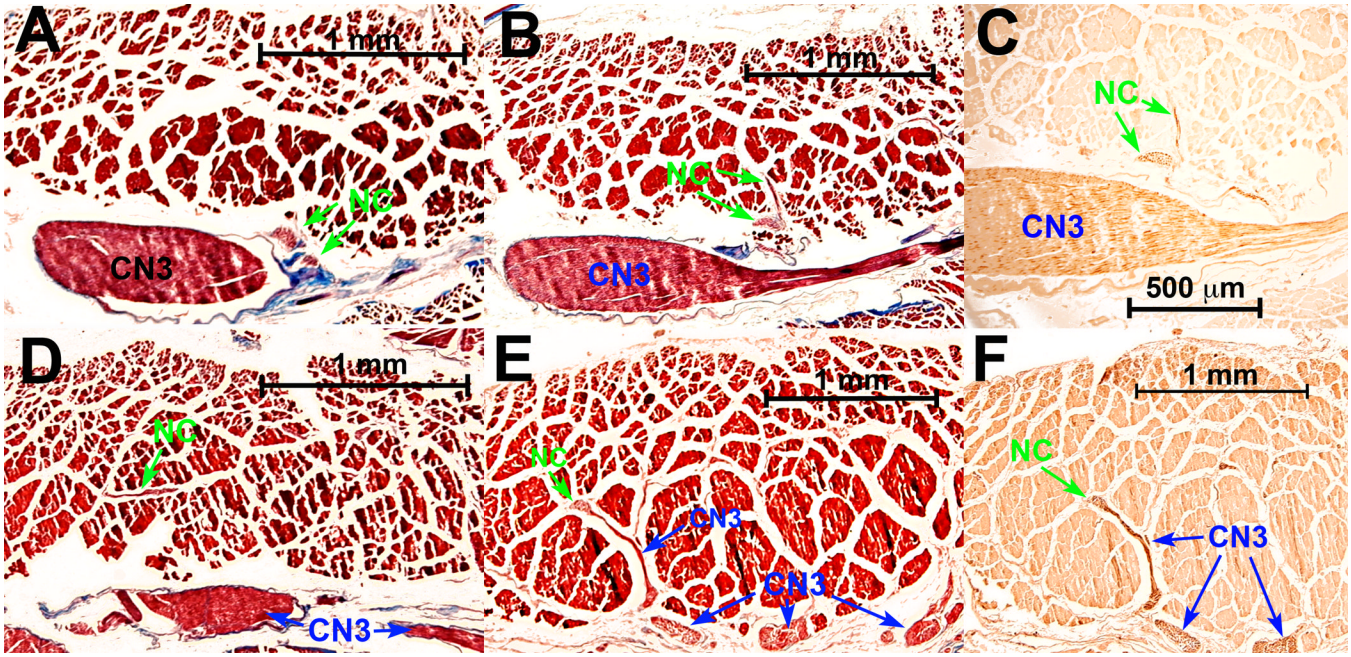

Fig. 6.

Transverse sections of rabbit superior rectus (SR) muscle, arranged from deep (A) to superficial (F). **A**. Two small nonclassical (NC) n branches coursed from the major oculomotor n (CN3) trunk proximal to its bifurcation into superior and inferior divisions 2.5 cm posterior to corneal surface. **B.** CN3 divided into superior and inferior divisions 200 μm anterior to A, but NC nn entered the EOM at this location. **C**. Immunohistochemistry of serial section 20 μm from B shows brown choline acetyltransferase (ChAT) reaction of CN3 and NC nn **D.** Small NC nn arborized within the SR 1 mm anterior to A. **E.** Anastomoses between NC n branch, cut transversely, and tangentially sectioned branches from principal CN3 trunk 3 mm anterior to A. F. Serial section 20 microns from E. shows by brown reaction product that NC and CN3 branches were immunoreactive for ChAT. Panels A, B, D, E – Masson trichrome.

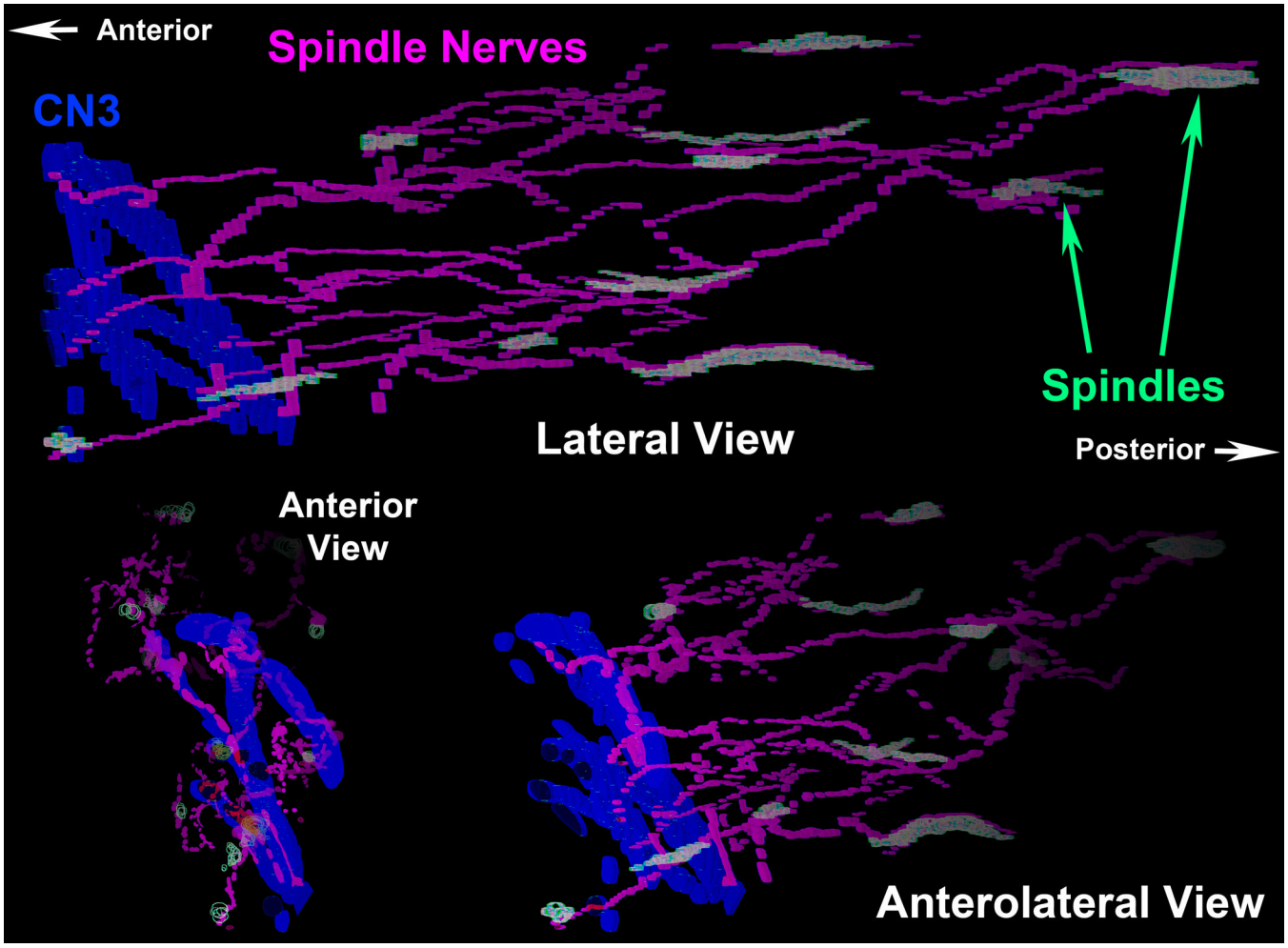

Fig. 7.
Three perspectives from a 3D reconstruction of deep portion of human inferior rectus (IR) muscle showing branches of classical CN3 motor n. in blue, nonclassical (NC) nn in magenta, and muscle spindles in light green. Note that the NC nn interconnect the spindles, and join with the classical CN3.

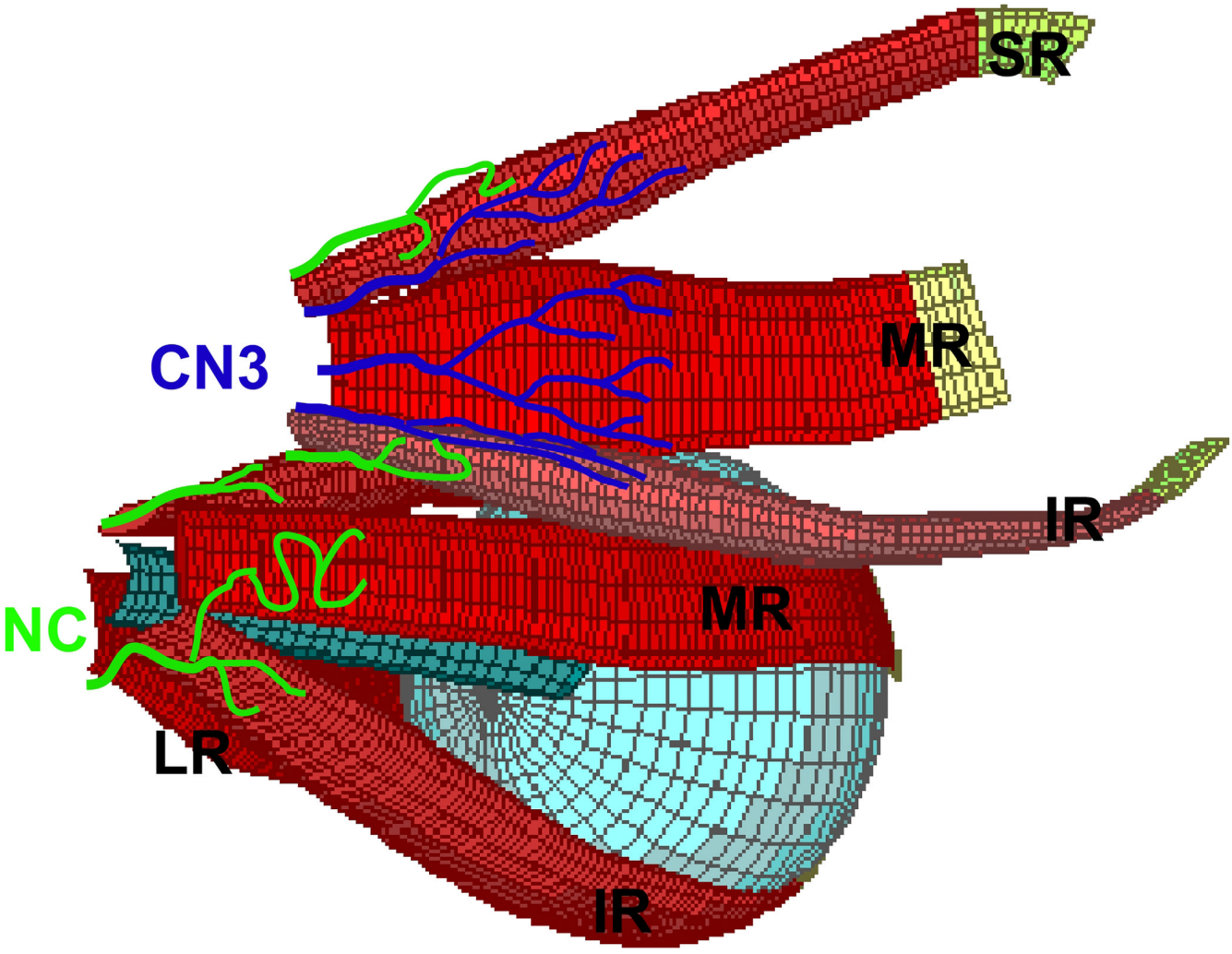

Fig. 8.

Diagrammatic illustration of classical oculomotor n. (CN3, blue) and non-classical (NC, green) innervation to EOMs. Branches of CN3 enter EOMs more anteriorly into the global surfaces of single EOMs, while NC nn enter more posteriorly from orbital surfaces, and may travel between EOMs. Right globe and both IO muscles rendered transparent. Abbreviations as in Fig. 1.